Synthesis, Structure, and Electronic Communication in Complexes Derived from $RC_2Co_2(CO)_6C_2Co_2(CO)_6R$

C. John McAdam, Noel W. Duffy, Brian H. Robinson,* and Jim Simpson*

Department of Chemistry, University of Otago, P.O. Box 56, Dunedin, New Zealand

Received April 10, 1996[⊗]

The loss of a $Co_2(CO)_6$ fragment and the formation of compounds of the type $RC{\equiv}CC_2Co_2(CO)_{6-n}[P(OMe)_3]_nR$ (n =1−3) is the main consequence of thermally-initiated substitution reactions of the diyne complexes $RC_2Co_2(CO)_6C_2Co_2(CO)_6R$ [R = Ph, Fc; Fc = (η^5-C_5H_4)Fe(η^5-C_5H_5)] with $P(OMe)_3$. Unstable $RC_2Co_2(CO)_{6-n}[P(OMe)_3]_nC_2Co_2(CO)_{6-m}$-$[P(OMe)_3]_mR$ (n = 0−2, m = 0, 1) complexes are isolated in low yield, under mild reaction conditions, or in electron transfer catalyzed (ETC) substitution reactions. Thermal reactions with bis(diphenylphosphino)methane (dppm) gave $RC{\equiv}CC_2Co_2(CO)_4$(dppm)R (R = Ph, Fc) and $PhC_2Co_2(CO)_4$(dppm)$C_2Co_2(CO)_4$(dppm)Ph (**9a**). These results highlight the steric requirements for these modules if they are to be incorporated in molecular arrays. The crystal and molecular structure of **9a** has been determined from X-ray data. The dppm ligands adopt μ-η^2 configurations, bridging both Co−Co bonds, and bind at equatorial sites. Square-wave, conventional oxidative voltammetry and spectroscopic data provide evidence for communication between the ferrocene and C_2Co_2 redox centers and, in **9a**, the first example of delocalization between individual C_2Co_2 redox centers in a phosphine derivative. **9a**$^+$ and **9a**$^{2+}$ have been characterized.

A major goal of our recent work has been to identify redox modules incorporating metal clusters which can be part of multicomponent, coherent arrays of technological interest. These cluster redox modules must promote long-range electronic communication via suitable connectors and provide a measure of stereochemical control. Polyynes have received considerable attention[1,2] as possible molecular connectors or bridges as they promote the formation of linear (molecular-wire) arrays[3] and their complexes with $Co_2(CO)_6$ units are well-known.[4−7] We have previously shown that interaction between cobalt carbonyl cluster systems is possible when the clusters are linked by unsaturated $(C{\equiv}C)_x$ bridges,[8] although, in the case of linked $CCo_3(CO)_9$ cluster systems, the interaction is attenuated by coordinating one alkyne unit to a $Co_2(CO)_6$ moiety. Electronic interaction between adjacent redox centers results in various electron-transfer responses.[9] However, the redox activity of alkyne dicobalt systems is limited by the fact that facile EC reactions accompany one-electron reduction to the radical anion,[10,11] while oxidation of the $C_2Co_2(CO)_6$ cluster unit is not observed within accessible potential ranges.[11,12] For the diyne complexes, $RC_2Co_2(CO)_6C_2Co_2(CO)_6R$, it was found[13] that cleavage of a $Co_2(CO)_6$ unit is the dominant EC process. The buildup of electron density in the polynuclear core, which accompanies the substitution reactions, leads to the conversion of the redox center from a reducible to a readily oxidizable center; the ease of oxidation and stability of the resulting cations increase with the degree of carbonyl replacement.[11,14−16] The degree of substitution of polynuclear metal carbonyls is greatest with phosphite and chelating ligands such as dppm.[11,15] An added advantage with polyynes is the ability to incorporate the ferrocenyl redox terminus as an electrochemical marker to measure the effectiveness of communication along the backbone. Ferrocenylbutadiyne complexes also exhibit nonlinear optical properties while biferrocene compounds and bis(ferrocenyl)-alkynes are recognized as classical systems for the study of intravalence charge-transfer phenomena involving a

[⊗] Abstract published in *Advance ACS Abstracts,* August 15, 1996.

(1) Biswas, M.; Mukherjee, A. *Adv. Polymer Sci.* **1994**, *115*, 89. Benniston, A. C.; Grosshenny, V.; Harriman, A.; Ziessel, R. *Angew Chem. Int. Ed. Engl.* **1995**, *34*, 1100.

(2) Beck, W.; Niemer, B.; Wieser, M. *Angew Chem., Int. Ed. Engl.* **1993**, *32*, 923.

(3) Lagow, R. J.; Kampa, J. J.; Wei, H.-C.; Battle, S. L.; Genge, J. W.; Laude, D. A.; Harper, C. J.; Bau, R.; Stevens, R. C.; Haw, J. F.; Munson, E. *Science* **1995**, *267*, 362. Bunz, U. H. F. *Angew Chem, Int. Ed. Engl.* **1994**, *33*, 1073. Coat, F.; Lapinte, C. *Organometallics* **1996**, *15*, 477.

(4) Johnson, B. F. G.; Lewis, J.; Raithby, P. R.; Wilkinson, D. A. *J. Organomet. Chem.* **1991**, *408*, C9.

(5) Lewis, J.; Lin, B.; Khan, M. S.; Al-Mandhary, M. R. A.; Raithby, P. R. *J. Organomet. Chem.* **1994**, *484*, 161.

(6) Lindsell, W. E.; Preston, P. N.; Tomb, P. J. *J. Organomet. Chem.* **1992**, *439*, 201.

(7) Magnus, P.; Becker, D. P. *J. Chem. Soc., Chem. Commun.* **1985**, 640. Rubin, Y.; Knoebler, C. B.; Diederich, F. *J. Am. Chem. Soc.* **1990**, *112*, 4966.

(8) Worth, G. H.; Robinson, B. H.; Simpson, J. *Organometallics* **1992**, *11*, 3863. Elder, S. M.; Robinson, B. H.; Simpson, J. *J. Organomet. Chem.* **1990**, *398*, 165.

(9) Geiger, W. E.; Connelly, N. G. *Adv. Organomet. Chem.* **1985**, *24*, 87. Bard, A. J.; Faulkner, L. R. *Electrochemical Methods: Fundamentals and Applications*; Wiley: New York, 1980.

(10) Arewgoda, C. M.; Rieger, P. H.; Robinson, B. H.; Simpson, J.; Visco, S. *J. Am. Chem. Soc.* **1982**, *104*, 5633. Casagrande, L. V.; Chen, T.; Rieger, P. H.; Robinson, B. H.; Simpson, J.; Visco, S. J. *Inorg. Chem.* **1984**, *23*, 2019.

(11) Arewgoda, C. M.; Robinson, B. H.; Simpson, J. *J. Am. Chem. Soc.* **1983**, *105*, 1893.

(12) Robinson, B. H.; Simpson, J. In *Paramagnetic Organometallic Species in Activation/Selectivity Catalysis;* Chanon, M., Ed; Kluwer: Dordrecht, The Netherlands, 1989, p 357.

(13) Osella, D.; Nervi, C.; Ravera, M.; Duffy, N. W.; McAdam, C. J.; Robinson, B. H.; Simpson, J. *Inorg. Chim. Acta* **1996**, *247*, 99.

(14) Colbran, S. B.; Robinson, B. H.; Simpson, J. *Organometallics* **1983**, *2*, 952. Dawson, P. A.; Robinson, B. H.; Simpson, J. *J. Chem. Soc., Dalton Trans.* **1979**, *176*, 2.

(15) Aggarwal, R. P.; Connelly, N. G.; Crespo, M. C.; Dunne, B. J.; Hopkins, P. M.; Orpen, A. G. *J. Chem. Soc., Chem. Commun.* **1989**, 33; *J. Chem. Soc., Dalton Trans.* **1992**, 655.

(16) Bond, A.; Dawson, P. A.; Peake, B. M.; Robinson, B. H.; Simpson, J. *Inorg. Chem.* **1977**, *16*, 2199.

S0276-7333(96)00276-2 CCC: $12.00

π-conjugated connector.[17,18] The work described in this paper is concerned with complexes of the diynes $RC_2Co_2(CO)_6C_2Co_2(CO)_6R$ (R = Ph, Fc) with phosphites and dppm and the effect of substitution on the electronic communication between the C_2Co_2 and Fc redox centers, taken as model precursors for larger arrays.

Results and Discussion

Reactions with $(MeO)_3P$. Attempts to thermally substitute the diyne complexes $RC_2Co_2(CO)_6C_2Co_2(CO)_6R$ [R = Ph (**1a**), Fc (**1b**)] with $P(OMe)_3$ led to the loss of one $Co_2(CO)_6$ unit, with substitution occurring at the remaining $C_2Co_2(CO)_6$ center to give the derivatives $RC{\equiv}CC_2Co_2(CO)_{6-n}[P(OMe)_3]_nR$ ($n = 1-3$) (**2**−**4**).

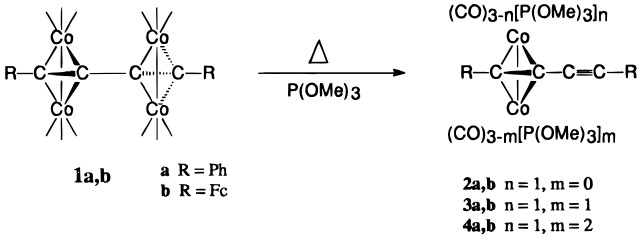

1a,b **a** R = Ph **b** R = Fc

2a,b n = 1, m = 0
3a,b n = 1, m = 1
4a,b n = 1, m = 2

The relative amounts of the derivatives were determined by the ratio of ligand to cluster, with formation of **4a,b** requiring a large excess of the phosphite. Small yields of the products $RC_2\{Co_2(CO)_5P(OMe)_3\}C_2\{Co_2(CO)_{6-n}[P(OMe)_3]_n\}R$, [R = Ph, $n = 0$, 1, 2, **5a**, **6a,**

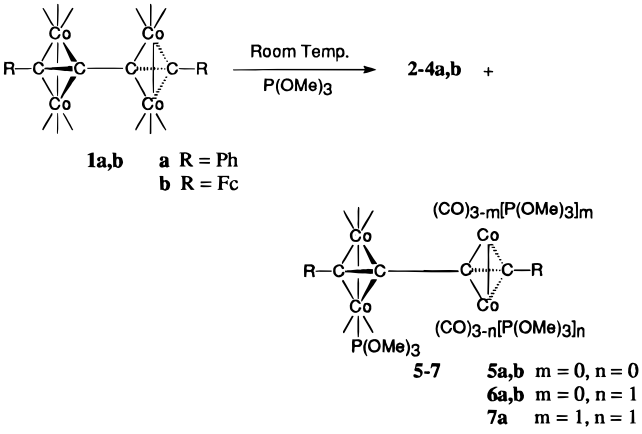

1a,b **a** R = Ph **b** R = Fc

5-7 **5a,b** m = 0, n = 0
6a,b m = 0, n = 1
7a m = 1, n = 1

7a; R = Fc, $n = 0$, 1, **5b, 6b**] were obtained at ambient temperature, but even under these mild conditions, products resulting from the extrusion of one of the $Co_2(CO)_6$ units predominated. Complexes **2a** and **3a** were red crystalline solids, but all others were isolated as oils, stable in air, soluble with variable stability in common organic solvents.

When **1a** was refluxed in benzene for 3 h, the bulk of the starting complex was recovered unchanged; there was no evidence for cleavage of a $Co_2(CO)_6$ fragment. Consequently, the coordination of at least one phosphite ligand is an essential first step in the loss of a dicobalt unit from the tetracobalt−diyne module. The isolation of a Co_4−diyne complex **9a** (*vide infra*) from the corresponding reaction with a bidentate phosphine dppm suggests that dissociation could be assisted by the coordination of a labile monodentate P-donor ligand to the adjacent Co_2−diyne center. Further support for this contention comes from the observation that **3a** can be

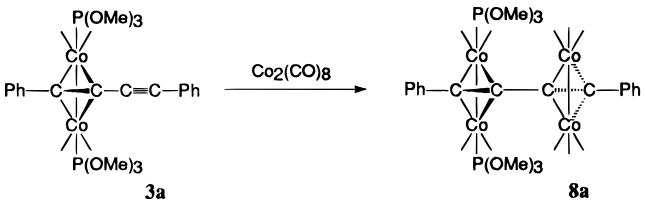

converted to **8a** in high yield, indicating that the steric requirements of the unsubstituted $Co_2(CO)_6$ fragment are not compromised, even by having two, axially substituted phosphite ligands on the adjacent cluster unit.

Loss of $Co_2(CO)_6$ therefore results from steric interactions between phosphite ligands coordinated to each of the adjacent cluster centers, a conclusion supported by the examination of models. Richmond and co-workers have recently[19] made related observations for reactions with phosphine anhydrides, and the loss of a single $Co_2(CO)_6$ moiety on methanolysis of the Si−H bond of $HSi[C_2Co_2(CO)_6SiMe_3]_3$ has been attributed[20] to steric crowding in the triply coordinated ethynylsilane.

ν(CO) spectra of **2**, **3**, and the symmetrically substituted **6** are similar to those of the corresponding $RC_2Co_2(CO)_{6-n}L_nR$ ($n = 1-3$) compounds[21−23] and show the characteristic reduction in the carbonyl stretching frequencies with increasing phosphite substitution. Experience with $RC_2Co_2(CO)_{6-n}L_nR$ molecules shows that, for $n = 1-2$, the ligand prefers an axial coordination site on each cobalt atom. The similarities in the spectra of the symmetrical Co_2− and Co_4−diyne derivatives indicate that they have the same ligand configuration while those of the unsymmetrically ligated **5**, **7a**, and **8a** are essentially a superposition of those of the individual $Co_2(CO)_{6-n}L_n/Co_2(CO)_{6-m}L_m$−diyne components. These conclusions are fully supported by the ^1H and ^{31}P NMR spectra. ^{31}P NMR spectra of **2, 3**, **5**, and **8** gave singlet resonances in the range 156−163 ppm while the coupling constant of $^3J_{P-H} = 11-12$ Hz for the methoxy protons in the ^1H NMR are similar to those observed in the spectra of other metal−carbonyl phosphite complexes.[21,22,24] Complexes **3, 7a, 8a** exhibited an $X_9AA'X'_9$ spin system in their ^1H NMR spectra consistent with diaxial substitution and previously observed for $H_2C_2Co_2(CO)_4(PMe_3)_2$.[25] The Co_4−diyne complex **6b** with a single phosphite substituent on each

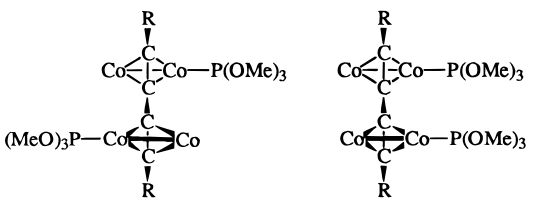

Isomers for **6**

off the C_2Co_2 centers gave well-resolved, overlapping doublets in the ^1H and ^{31}P NMR indicating the presence of two isomers; ^1H NMR of **6a** also gave spectra for the

(17) Green, M. L. H.; Marder, S. R.; Thompson, M. E.; Bandy, J. A.; Bloor, D.; Kolinsky, P. V.; Jones, R. J. *Nature (London)* **1987**, *330*, 360. Yuan, Z.; Taylor, N. J.; Sun, Y.; Marder, T. B.; Williams, I. D.; Cheng, L.-T. *J. Organomet. Chem.* **1993**, *449*, 27.

(18) Kaufman, F.; Cowan, D. O. *J. Am. Chem. Soc.* **1970**, *92*, 6198. Bunel, E. E.; Valle, L.; Jones, N. L.; Carroll, P. J.; Gonzalez, M.; Munoz, N.; Manriquez, J. M. *Organometallics* **1988**, *7*, 789.

individual isomers but only a broad ^{31}P resonance. With individual ligands coordinated to an axial site on the C_2Co_2 unit, isomerism would arise by substitution at the two alternative axial sites defined by the diyne backbone. Integration indicated that the isomer ratio was 1:1 for **6a** and 2:1 for **6b**; the difference may reflect the steric influence of the bulky ferrocenyl alkyne substituent.

Substitution of three phosphite ligands as in **4a**,**b** requires that one Co_2 module will have at least one ligand occupying an equatorial site. As a consequence, two discrete sets of ^1H and ^{31}P resonances in a 2:1 ratio are observed, but in the case of **4b** they are very broad over the temperature range 203−298 K. Steric congestion from the Fc terminii in **4b** is the most likely cause of the increased ligand lability in **4b** compared to **4a**.

Electron Transfer Catalyzed Substitution Reactions. Electron transfer catalyzed (ETC) initiation[11,12] of CO substitution in **1a,b** conceptually provides milder

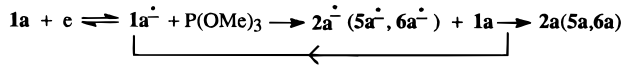

reaction conditions which may avoid the loss of a $Co_2(CO)_6$ unit during substitution. ETC reactions have not been studied for systems where there are interacting redox centers. Electrochemical investigations of the parent **1a** revealed a primary two-electron reduction process, which could be resolved at low temperatures into individual reversible one electron waves.[13] These observations were consistent with the discrete reduction of the two C_2Co_2 redox centers so each $C_2Co_2(CO)_6$ moiety of **1** should act as a substrate for ETC substitution reactions. Benzophenone ketyl (BPK) initiated ETC reactions with **1** were found to be complete within 1 min at ambient temperature yielding a mixture of complexes with a single phosphite substituent on one or both of the dicobalt units, ie, **2, 5,** and **6.** The observation that complexes with a single phosphite substituent per C_2Co_2 center are the major products is consistent with our experience with the monoyne systems.[12]

For **1a** the dominant chemical reaction once the radical anion is formed is the loss of one $Co_2(CO)_6$ group, and this will provide the route to $\mathbf{2a}^{\bullet-}$. Electrochemical and ESR studies of alkynedicobalt hexacarbonyl systems have shown that, unless the alkyne substituent is strongly electron withdrawing, reduction of $C_2Co_2(CO)_{6-n}L_n$ unit is followed by facile loss of $Co(CO)_{4-n}L_n^-$ to produce mononuclear cobalt radicals, which in turn decompose to, *inter alia*, the free alkyne.[10,11,26] Ph or Fc alkyne substituents are not electron-withdrawing groups. Consequently, it is not possible to distinguish between a direct ETC route to **5** and one where **2** reacts with $Co(CO)_{4-n}L_n^-$ from decomposition from the radical anion.

Reactions with dppm. **1a** reacted smoothly with dppm to give $PhC_2Co_2(CO)_4(dppm)C_2Co_2(CO)_4(dppm)Ph$ (**9a**).

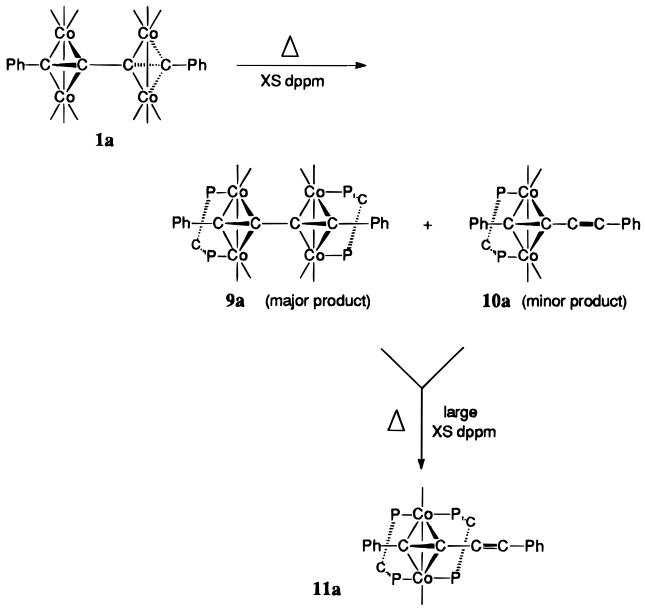

In contrast to the reactions with $P(OMe)_3$, **10a**, which results from the loss of a $Co_2(CO)_6$ fragment, was only a minor product. Attempts to further substitute **9a** by a reaction with a large excess of dppm led to the loss of one Co_2 unit and the formation of **11a**. Structural studies[27,28] have shown that chelation of dppm to Co_2−alkynes forces an equatorial rather than axial ligation. This may explain the higher yields of the Co_4−diyne product.

Reaction of **1b** with dppm led *exclusively* to the loss of one $Co_2(CO)_6$ fragment and the formation of $FcC{\equiv}CC_2$-

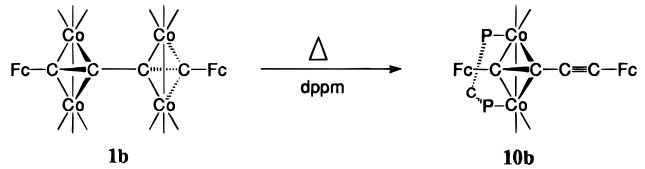

$Co_2(CO)_4(dppm)Fc$ (**10b**) and $Co_4(CO)_8(dppm)_2$.[29] Presumably the greater steric requirements of the ferrocenyl alkyne substituents force the molecule to lose $Co_2(CO)_6$ in the substitution process.

ν(CO) spectra of **9a,** and **10a**,**b**, are comparable to Co_2−alkyne analogues,[15,21,27,30] and the single ^{31}P NMR resonances in the range 38−40 ppm suggest that the coordination preference of the bidentate ligand is to μ-η^2 bridge the Co−Co bond. This assignment was confirmed for **9a** by an X-ray structural determination. Two

(19) Richmond, M. University of Texas, personal communication.
(20) Corriu, R. J. P.; Moreau, J. J. E.; Praet, H. J. *J. Organomet. Chem.* **1989**, *376*, C39.
(21) Chia, L. S.; Cullen, W. R.; Franklin, M.; Manning, A. R. *Inorg. Chem.* **1975**, *14*, 2521.
(22) Harper, M.; McAdam, C. J.; Robinson, B. H.; Simpson, J. Unpublished observations. Duffy, N. W.; McAdam, C. J.; Robinson, B. H.; Simpson, J. *J. Organomet. Chem.*, manuscript in preparation.
(23) Varadi, G.; Vizi-Orsosz, A.; Vastag, S.; Palyi, G. *J. Organomet. Chem.* **1976**, *108*, 225.
(24) Church, M. J.; Mays, M. J. *J. Inorg. Nucl. Chem.* **1971**, *33*, 253.
(25) Bonnet, J.-J.; Mathieu, R. *Inorg. Chem.* **1978**, *17*, 1973.
(26) Dickson, R. S.; Peake, B. M.; Rieger, P. H.; Robinson, B. H.; Simpson, J. *J. Organomet. Chem.* **1979**, *172*, C63.
(27) Bird, P. H.; Fraser, A. R.; Hall, D. N. *Inorg. Chem.* **1977**, *16*, 1923.
(28) Downard, A. J.; Robinson, B. H.; Simpson, J. *J. Organomet. Chem.* **1993**, *447*, 281.
(29) Lisic, E. C.; Hanson, B. E. *Inorg. Chem.* **1986**, *25*, 812.
(30) Downard, A. J.; Robinson, B. H.; Simpson, J. *Organometallics* **1986**, *5*, 1122. Farrar, D. H.; Payne, N. C. *Inorg. Chem.* **1981**, *20*, 821. Cunninghame, R. G.; Hanton, L. R.; Jensen, S. D.; Robinson, B. H.; Simpson, J. *Organometallics* **1987**, *6*, 1470. Jensen, S. D.; Robinson, B. H.; Simpson, J. *Organometallics* **1987**, *6*, 1479.

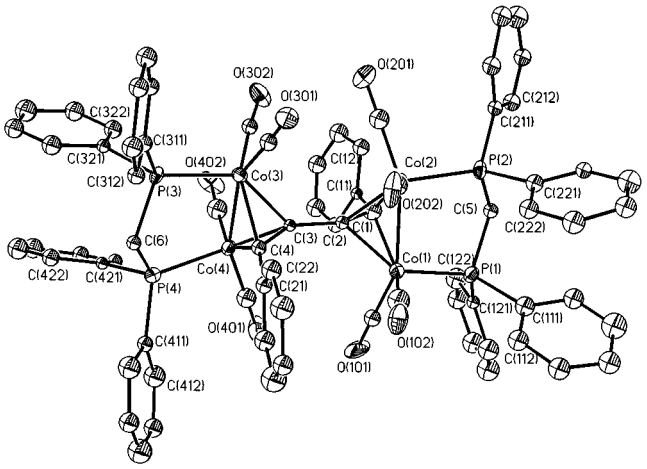

Figure 1.

^{31}P resonances at 40 and 44 ppm were observed for **11a**, consistent with endo and exo coordination of the dppm (with respect to the diyne chain).

No ETC-initiated reactions were carried out with dppm because earlier investigations had shown that ETC reactions of cobalt cluster systems with bidentate ligands were complicated by the ready formation of products with pendant donor atoms or where the bidentate ligand formed a bridge between two cluster units.[30]

X-ray Structural Determination of 9a. The detailed structure of **9a** was examined by X-ray crystal structure analysis. A perspective view of the molecule is shown in Figure 1, which also defines the atom-numbering scheme, with selected bond length and angle information in Table 1. The structure consists of discrete molecules with the closest intermolecular contact being 3.22(3) Å between C(214) and O(102). The molecule consists of two approximately tetrahedral (μ-alkyne)dicobalt cores, typical of perpendicular alkyne complexes,[31] with the interline angles C(1)−C(2)/Co(1)−Co(2) 90(1)° and C(3)−C(4)/Co(3)−Co(4) 89.8(8)°, respectively. The C_2Co_2 units are coordinated to the diyne in a *trans* configuration and linked by a single bond between C(2) and C(3). The outer C atoms of the diyne chain, C(1) and C(4), carry phenyl substituents also orientated *trans* to each other. Each cobalt atom has one "axial" and one "pseudo-equatorial" CO ligand and a P donor atom from the dppm ligand in the alternative equatorial site. Both dppm ligands adopt μ-η^2 coordination, bridging the Co−Co bonds, and the non-acetylene ligands adopt the classical "sawhorse" arrangement with respect to the cobalt atoms in each C_2Co_2 unit.[32] The solid-state arrangement of the bridging dppm ligands is such that they are directed away from the central portion of the molecule, a configuration that minimizes repulsive interactions between the $C_2Co_2(CO)_2$(dppm) moieties. This contrasts sharply with the orientation adopted[5] by the complex $\{Me_3SiC_2[Co_2(CO)_4(dppm)]C{\equiv}C-\}_2$, where the dppm ligands are coordinated to the alternative equatorial sites to those used in **9a** with one phenyl ring from each P atom directed toward the center of the alkyne chain. This orientation is clearly made possible by the increased length of the alkyne chain which allows a more compact disposition of the dppm ligands.

The overall structure resembles those of the parent diynes **1** (R = Me_3Si[7] and Ph[4]), with the two $C_2Co_2(CO)_2$(dppm) units linked via a short 1.44(2)Å C−C single bond between two carbyne C atoms, suggesting a degree of electron delocalization along the backbone. The alkyne C−C bonds are much shorter, C(1)−C(2) 1.36(3) Å and C(3)−C(4) 1.33(2) Å, and are in reasonable agreement with those found in the unsubstituted tetracobalt diynes, although the esd's in this structure are somewhat high. However, in this molecule, the Co−C distances within the two C_2Co_2 tetrahedra are equal within experimental error and do not display the marked tilting of the C−C vectors toward the central C(2) and C(3) atoms observed in **1a**.[4] The *cis*-bent configuration of the individual alkyne units is retained, as anticipated for perpendicular acetylenes;[25] however

Table 1. Selected Bond Lengths (Å) and Angles (deg) for 9a

C(11)−C(1)	1.49(3)	C(1)−C(2)	1.36(3)
C(1)−Co(2)	1.94(2)	C(1)−Co(1)	1.95(2)
C(2)−C(3)	1.44(2)	C(2)−Co(1)	1.94(2)
C(2)−Co(2)	1.94(2)	C(3)−C(4)	1.33(2)
C(3)−Co(3)	1.94(2)	C(3)−Co(4)	1.97(2)
C(4)−C(21)	1.44(2)	C(4)−Co(3)	1.96(2)
C(4)−Co(4)	1.99(2)	Co(1)−C(101)	1.73(2)
C(101)−O(101)	1.17(2)	Co(1)−C(102)	1.75(2)
C(102)−O(102)	1.16(2)	Co(1)−P(1)	2.206(6)
Co(1)−Co(2)	2.469(4)	P(1)−C(111)	1.83(2)
P(1)−C(121)	1.80(2)	P(1)−C(5)	1.84(2)
C(5)−P(2)	1.81(2)	Co(2)−P(2)	2.209(6)
P(2)−C(211)	1.82(2)	P(2)−C(221)	1.82(2)
Co(2)−C(201)	1.72(2)	C(201)−O(201)	1.17(2)
Co(2)−C(202)	1.80(2)	C(202)−O(202)	1.14(2)
Co(3)−Co(4)	2.438(4)	Co(3)−C(301)	1.79(2)
C(301)−O(301)	1.12(2)	Co(3)−C(302)	1.77(2)
C(302)−O(302)	1.15(2)	Co(3)−P(3)	2.209(6)
P(3)−C(6)	1.80(2)	P(3)−C(311)	1.85(2)
P(3)−C(321)	1.86(2)	C(6)−P(4)	1.83(2)
Co(4)−P(4)	2.220(6)	P(4)−C(411)	1.81(2)
P(4)−C(421)	1.84(2)	Co(4)−C(401)	1.72(2)
C(401)−O(401)	1.17(2)	Co(4)−C(402)	1.71(2)
C(402)−O(402)	1.18(2)		

C(2)−C(1)−C(11)	128(2)	C(2)−C(1)−Co(2)	69.8(11)
C(2)−C(1)−Co(1)	69.1(11)	Co(2)−C(1)−Co(1)	78.9(7)
C(1)−C(2)−Co(1)	70.1(12)	C(1)−C(2)−C(3)	143(2)
C(3)−C(2)−Co(1)	134.5(12	C(1)−C(2)−Co(2)	69.3(11)
C(3)−C(2)−CO(2)	132.9(13)	Co(1)−C(2)−Co(2)	79.0(6)
C(4)−C(3)−C(2)	141(2)	C(2)−C(3)−Co(3)	134.2(12)
C(4)−C(3)−Co(3)	71.0(10)	C(2)−C(3)−Co(4)	134.7(12)
C(4)−C(3)−Co(4)	71.1(10)	Co(3)−C(3)−Co(4)	77.2(6)
C(3)−C(4)−C(21)	136(2)	C(3)−C(4)−Co(3)	69.2(10)
C(3)−C(4)−Co(4)	69.7(10)	Co(3)−C(4)−Co(4)	76.2(6)
C(101)−Co(1)−C(102)	102.0(9)	C(2)−Co(1)−C(1)	40.8(7)
C(101)−Co(1)−P(1)	95.3(6)	C(102)−Co(1)−P(1)	108.9(7)
C(101)−Co(10)−Co(2)	152.9(6)	O(101)−C(101)−Co(1)	179(2)
C(102)−Co(1)−Co(2)	95.9(7)	O(102)−C(102)−Co(1)	176(2)
P(1)−Co(1)−Co(2)	98.0(2)	C(5)−P(1)−Co(1)	107.9(6)
P(2)−C(5)−P(1)	108.7(9)	C(201)−Co(2)−C(202)	94.3(9)
C(2)−Co(2)−C(1)	40.9(7)	C(201)−Co(2)−P(2)	99.9(7)
C(202)−Co(2)−P(2)	108.3(6)	C(201)−Co(2)−Co(1)	152.4(6)
O(201)−C(201)−Co(2)	179(2)	C(202)−Co(2)−Co(1)	103.1(6)
O(202)−C(202)−Co(2)	175(2)	C(1)−Co(2)−Co(1)	50.8(6)
C(2)−Co(2)−Co(1)	50.4(5)	P(2)−Co(2)−Co(1)	94.9(2)
C(5)−P(2)−Co(2)	109.0(6)	C(302)−Co(3)−C(301)	97.9(8)
C(3)−Co(3)−C(4)	39.9(7)	C(301)−Co(3)−P(3)	97.8(6)
C(302)−Co(3)−P(3)	111.0(6)	C(301)−Co(3)−Co(4)	151.9(6)
O(301)−C(301)−Co(3)	177(2)	C(302)−Co(3)−Co(4)	101.4(6)
O(302)−C(302)−Co(3)	174(2)	P(3)−Co(3)−Co(4)	94.1(2)
C(6)−P(3)−Co(3)	109.0(6)	P(3)−C(6)−P(4)	109.8(9)
C(402)−Co(4)−C(401)	97.6(9)	C(3)−Co(4)−C(4)	39.2(6)
C(402)−Co(4)−P(4)	106.0(7)	C(401)−Co(4)−P(4)	99.8(7)
C(401)−Co(4)−Co(3)	156.4(7)	O(401)−C(401)−Co(4)	174(2)
C(402)−Co(4)−Co(3)	91.4(7)	O(402)−C(402)−Co(4)	177(2)
C(3)−Co(4)−Co(3)	50.8(5)	C(4)−Co(4)−Co(3)	51.3(5)
P(4)−Co(4)−Co(3)	98.7(2)	C(6)−P(4)−Co(4)	108.6(6)

(31) Hoffman, D. M.; Hoffmann, R.; Fisel, C. R. *J. Am. Chem. Soc.* **1982**, *104*, 3858.
(32) Gregson, D.; Howard, J. A. K. *Acta Crystallogr.* **1983**, *C39*, 1024.

the angles subtended at the "external" alkyne C atoms, C(11)−C(1)−C(2) 128(2)° and C(21)−C(4)−C(3) 136(2)°, are lower than the corresponding angles at the C atoms linking the C_2Co_2 cores, C(1)−C(2)−C(3) 143(2)° and C(2)−C(3)−C(4) 141(2)°. The analogous complex $Ph_2C_2Co_2(CO)_4(dppm)$[27] displays similar differences in the bend back angles which may be a steric consequence of the bridging dppm ligands. In contrast, the corresponding angles for the less sterically challenged tetrayne complex are similar, 147.0(7)° at the external and 144.4(9)° at the internal alkyne carbon atoms.

The Co−Co bond lengths, Co(1)−Co(2) 2.469(4) Å and Co(3)−Co(4) 2.438(4) Å, are unusual in that the coordination of the dppm ligands has resulted in a significant contraction of one of the of the Co−Co vectors when compared with the unsubstituted complexes (Co−Co: 2.461 Å, R = Ph; 2.474 Å, R = Me_3Si). Alkyne dicobalt complexes with a single dppm bound in a μ-η^2 fashion[27,33,34] also show Co−Co bond distances in the range 2.46−2.47 Å; for example d(Co−Co) in $Ph_2C_2Co_2(CO)_4(dppm)$[27] is 2.459(2) Å. This contrasts sharply with observations of significant lengthening of the Co−Co vectors on μ^2 coordination of a bidentate ligand to a single cobalt[21,35] atom in the alkyne dicobalt core or on the substitution of a second μ-η^2 dppm phosphite ligand to an alkyne dicobalt cluster.[15] In addition to the short Co−Co bond, the coordination geometry around the Co(3) and Co(4) atoms deviates more from the idealized "sawhorse" configuration than for the other Co_2C_2 unit. The torsion angles C(101)−Co(1)−Co(2)−C(201), −1(2)°, P(1)−Co(1)−Co(2)−P(2), −4.3(2)°, and C(102)−Co(1)−Co(2)−C(202), −4.3(9)°, show that the pseudoequatorial substituents on the Co(1) and Co(2) atoms are close to the anticipated eclipsed conformation, whereas deviation from the eclipsed geometry is evident from the corresponding figures for the second cluster unit, C(301)−Co(3)−Co(4)−C(401), −38(2)°, P(3)−Co(3)−Co(4)−P(4), −12.3(2)°, and C(302)−Co(3)−Co(4)−C(402), −18(1)°. These observations indicate that the observed compression of the Co(3)−Co(4) bond is most likely to be the result of steric rather than electronic influences with the effect limited to one Co_2C_2 unit.

Redox Chemistry. For the complexes **2**−**11** the $C_2Co_2(CO)_{6-n}L_n$ redox centers display either reduction or oxidation processes in their electrochemical responses depending on the number of carbonyl groups substituted by the phosphine ligand. The parent diyne[13] and $RC_2Co_2(CO)_{6-n}L_n$ complexes undergo complicated fast ECE reactions following the formation of radical anions, which leads to the loss of $Co_2(CO)_6$ and/or Co−Co bond cleavage. These fast ECE processes are even more complicated for **2**−**11**. Reduction electrochemistry therefore provided little information on the electronic structure of these complexes and will not be discussed further. Oxidation processes for individual $[C_2Co_2(CO)_{6-n}L_n]$ redox centers were more amenable to study. The primary electrochemical process for each redox center is the formation of a radical cation $[C_2Co_2(CO)_{6-n}L_n]^{\bullet+}$. Potentials for the couples $[C_2Co_2(CO)_{6-n}L_n]^{+/0}$ follow a consistent pattern depending on the value of n and selected data are given in Table 2. As expected, with an increase in the number of $P(OMe)_3$ ligands per redox center the potential decreases and the chemical reversibility of the couple increases (reversibility is only seen at high scan rates and/or low temperatures for **3a,b** and **4a,b)** (Figures 2 and 3). For **2b**−**4b** the $[Fc]^{+/0}$ couple of the alkyne substituent has a lower potential than the $[C_2Co_2(CO)_{6-n}L_n]^{+/0}$ couple (Figure 3).

Table 2 [a]

		$C_2Co_2(CO)_xP_{6-x}$ [c]		ferrocenyl [c]	
compd	E_{pc}^{red} [b]	$E_1°$ (i^a/i^c)	$E_2°$ (i^a/i^c)	$E_1°$ (i^a/i^c)	$E_2°$ (i^a/i^c)
1a	−0.94				
1b	−1.16			0.38 (0.9)	0.44 (1.0)
2a	−0.73	0.89	1.27[b]		
2b	−1.1	1.30		0.47 (0.96)	0.64 (0.94)
3a		0.69 (0.43)			
		0.684 (1.0)[d]			
3b		0.98 (0.4)		0.36 (0.94)	0.61 (0.91)
		0.98 (0.95)[d]			
9a		0.432 (1.0)	0.880 (1.0)		
10a	−1.25	0.67 (0.9)			
10b	−1.04	1.061 (0.93)		0.385 (0.97)	0.599 (0.99)
11a		0.162 (1.0)	1.02[b]		

[a] All data are referenced to SCE with Fc* at −0.076 V and Fc at 0.478 V, CH_2Cl_2, scan rate 100 mV s^{-1}, TBAH (0.1 M), Pt electrode. [b] Electron transfer is not chemically reversible. [c] Location of redox center, oxidation process. [d] Values in italics at 2 V s^{-1}

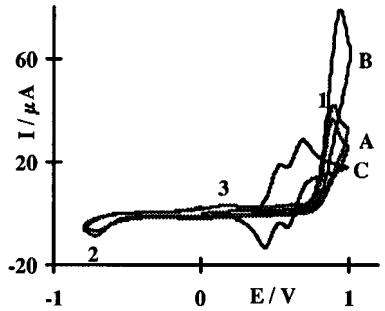

Figure 2. Cyclic voltammetry of **2a** (0.8 mM) at 400 mV s^{-1} (A, $E_{p1}^a = 0.89$, $E_{p2}^c = -0.73$, and $E_{p3}^a = 0.18$ V) and 2 V s^{-1} (B, $E_p^a = 0.91$ V) and **2b** at 200 mV s^{-1} showing two of the three oxidations (C, $E^1_{1/2} = 0.47$ V, $E^2_{1/2} = 0.64$ V, and $E^3_{1/2} = 1.3$ V) (CH_2Cl_2).

Communication between individual ferrocenyl redox centers in **1b** was identified in the electrochemistry by resolution of the single response at 0.41 V at 20 °C into $E°$[**1b**]$^{+/0}$ and $E°$[**1b**]$^{2+/+}$ at −20 °C with a separation of 35 mV.[13] On this basis the two one-electron reversible oxidation processes found for **2b** ($E° = 0.49$ and 0.55 V) and **3b** ($E° = 0.44$ and 0.56 V) can be assigned to the ferrocenyl redox center. As the ferrocenyl terminii are structurally nonequivalent in **2b** and **3b**, discrete $[Fc]^{+/0}$ couples are expected for each substituent. The most negative couple for **2b** and **3b** is assigned to $[Fc]^{+/0}$ for the ferrocenyl group adjacent to the electron-rich ligand-substituted cluster, and the other couple, which differ by 0.05 V between **2b** and **3b**, to $[Fc]^{+/0}$ adjacent to the unsubstituted cluster. A partially reversible wave for oxidation of the $[C_2Co_2(CO)_{6-n}L_n]$ units occurs at $E_p^a = \sim 1.3$ and 0.95 V for **2b** and **3b** respectively; for the phenyl analogues **2a** and **3a** oxidation occurs at $E_p^a = 0.90$ and 0.69 V. The large difference in potentials for the third oxidation process is due to the electron-withdrawing effect of the oxidized ferrocenyl terminii.

(33) Gelling, A.; Jeffery, J. C.; Povey, D. C.; Went, M. J. *J. Chem. Soc. Chem. Commun.* **1991**, 349.
(34) Nicolaou, K. C.; Maligres, P.; Suzuki, T.; Wendeborn, S. V.; Dai, W. M.; Chadha, R. K. *J. Am. Chem. Soc.* **1992**, *114*, 8890.
(35) Bianchini, C.; Dapporto, P.; Mela, A. *J. Organomet. Chem.* **1979**, *174*, 205.

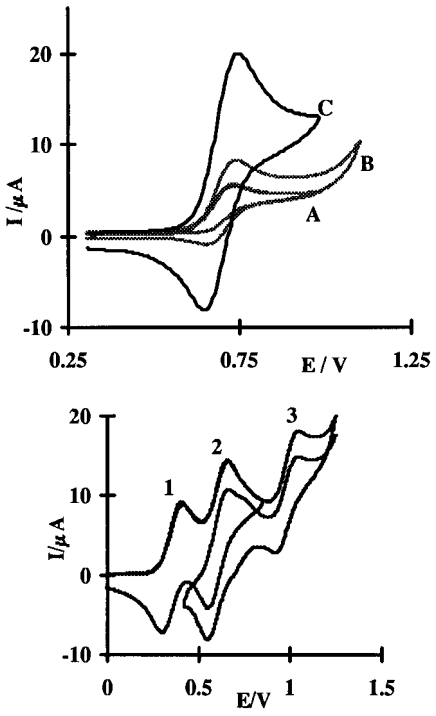

Figure 3. (a) Top: Cyclic voltammetry of **3a** (1 mM) at (A) 50 (0.0), (B) 100 (0.43), and (C) 1000 (0.89) mV s^{-1} (I^c/I^a) (CH_2Cl_2) (b) Bottom: Cyclic voltammetry of **3b** (0.6 mM) at 200 mV s^{-1} showing the three oxidation processes (CH_2Cl_2).

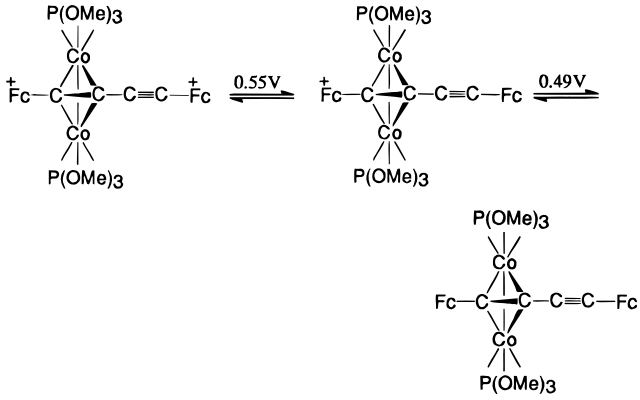

Dppm derivatives provided definitive evidence for strong interaction between cluster redox centers, and this was investigated by square-wave voltammetry and OTTLE spectroscopy, as well as conventional techniques. Complexes **10** provide an interesting comparison with **3** as they have the same number of donor atoms per Co_2 unit. Chelation by dppm reduces the lability of the coordinated ligand imparting chemical reversibility to the system (Figure 4) but little change in potential despite the more effective donation from a chelated phosphine ligand; thus $E°[\mathbf{10a}]^{+/0} = 0.67$ V and $E°[\mathbf{3a}]^{+/0} = 0.69$ V. Complex **10b** displays three chemically reversible couples (Figure 4) as there are nonequivalent ferrocenyl terminii plus the cluster redox center; assignments are shown below. In contrast, coordination of a *second* dppm ligand on a cluster subunit lowers the potential to the extent that $[\mathbf{11a}]^{+/0}$ is one of the lowest for the oxidation of phosphine-substituted clusters. Chemical reversibility is maintained for $[\mathbf{11a}]^{+/0}$ even though there is considerable steric congestion in the $Co_2(CO)_2(dppm)_2$ unit.

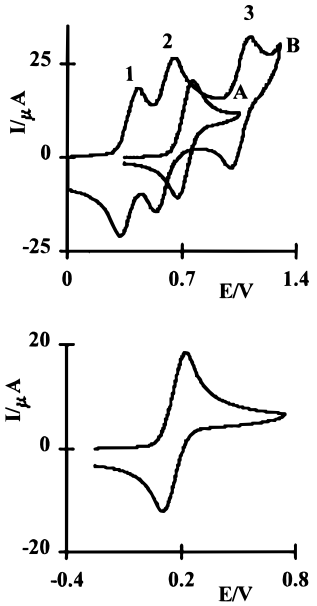

Figure 4. (a) Top: Cyclic voltammetry of **10a** (0.66 mM) and **10b** (0.73 mM) at 200 mV s^{-1} (CH_2Cl_2). (b) Bottom: Cyclic voltammetry of **11a** (0.8 mM) at 200 mV s^{-1} (CH_2Cl_2).

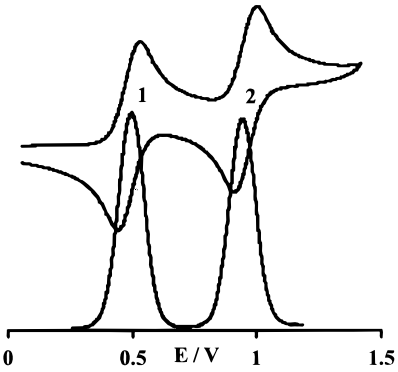

Figure 5. Cyclic (200 mV s^{-1}) and SQW (60 Hz, 25 mV) voltammograms of **9a** (1.2 mM). Results: Fitted SQW; $E^1_{1/2} = 0.420$ V, $E^2_{1/2} = 0.862$ V, $I_p{}^1/I^2_p = 1.0$, $\alpha^1 = \alpha^2 = 0.5$, $\log(\kappa t_p{}^{1/2}) = -0.2$, $\Delta E = 0.448$ V. Observed SQW: $E^1_{1/2} = 0.423$ V, $E^2_{1/2} = 0.864$ V, $I_p{}^1/I^2_p = 1.0$, $\Delta E = 0.447$ V. Observed CV: $\Delta E_p{}^1 = 83.5$ mV, $\Delta E_p{}^2 = 83.4$ mV, $I_p{}^a/I^c_p = 1.0$, $\Delta E = 0.449$ V (CH_2Cl_2).

The molecule which clearly shows communication and delocalization between the component redox centers is **9a**. Two chemically reversible oxidation waves, separated by 448 mV, were observed in the cyclic voltammograms for this symmetrical complex in which one dppm ligand is coordinated each Co_2 unit (Figure 5). The voltammetry was similar at all scan rates between 50 mV s^{-1} and 10 V s^{-1} and i_p vs $v^{1/2}$ plots were linear fulfilling the requirements for diffusion controlled one-electron processes establishing that $\mathbf{9a}^+$ and $\mathbf{9a}^{2+}$ are persistent on the electrochemical time scale. Square-wave voltammetry requires the synchronous application of a periodic square wave on a monotonic potential progression,[36] with current sampling, on a well-defined time scale. It is an effective technique because the response is not affected by non-Faradaic currents. Appropriate parameters for the diyne systems were found to be 60 Hz with an amplitude of 25 mV at

(36) Christie, J. H.; Turner, J. A.; Osteryoung, R. A. *Anal. Chem.* **1977**, *49*, 1899.

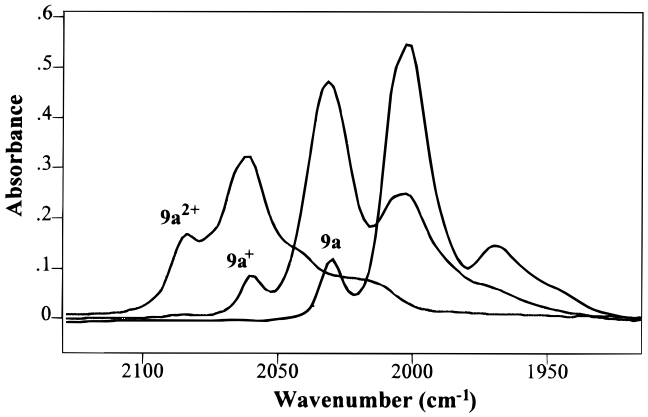

Figure 6. ν(CO) spectra in CH_2Cl_2 for **9a**, $\mathbf{9a}^+$, and $\mathbf{9a}^{2+}$.

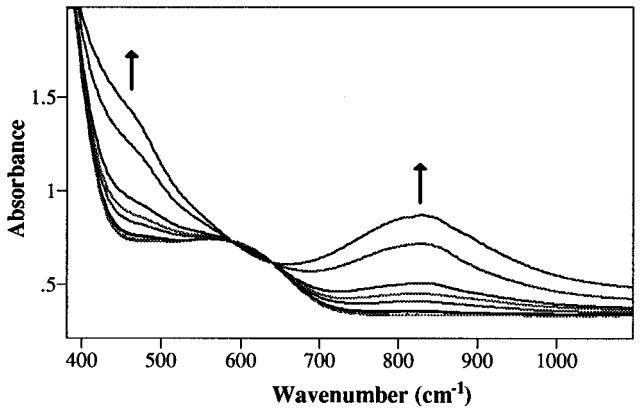

Figure 7. UV/vis OTTLE experiment from 380 to 1120 nm (0.7 mm path length) for **9a** (1.3 mM in 0.5 M (TBA)-PF_6/CH_2Cl_2) at increments of 0.1 V from 0.0 and 2.0 V and at −1.0 V: Neutral, λ_{max} (ϵ)/nm = 590 (3125); fully oxidized, λ_{max} = 450 (6240), 834 (3630).

increments of 1 mV. Kinetic parameters were obtained from experimental data by fitting the data using the COOL algorithm, and this proved to be an effective means of deconvoluting the redox processes. A square-wave voltammetric investigation of **9a** provided independent confirmation that each oxidation step was both reversible and one-electron (Figure 5). Square-wave analysis clearly showed that there were no preceding chemical reactions and the kinetic parameters were close to Nernstian [$\alpha^1 = \alpha^2 = 0.5$, $\log(\kappa t_p^{1/2}) = -0.2$]. Assignment of the two couples at 0.495 and 0.942 V is respectively $E°[\mathbf{9a}]^{+/0}$ and $E°[\mathbf{9a}]^{2+/+}$; K_c for conproportionation is 4×10^7. It is important to note that the weighted mean potential of these couples is $\sim E°[\mathbf{10a}]^{+/0}$.

Although the separation between $E°[\mathbf{9a}]^{+/0}$ and $E°[\mathbf{9a}]^{2+/+}$ is larger than that for **1a** (220 mV) it is well-known that the separation cannot be used as a definitive measure of delocalization without supporting spectral evidence, as structural reorganization, solvation, and ion pairing effects play a role. For example, for the biferrocene and [2,2]ferrocenophane-1,13-diyne the separation is 0.35 and 0.355 V, respectively, but the cation of the former is described as a localized species[37] and the latter as a delocalized mixed-valence species.[38] Two reasons to account for this have been cited, the proximity of the iron atoms and the fused π-ligand system. Nevertheless, the 450 mV separation for **9a** species suggests a significant Coulombic interaction compatible with a delocalized system via the diyne bridge, a conclusion supported by the spectroscopic work. Stoichiometric chemical oxidation of **9a** in CH_2Cl_2 produced $\mathbf{9a}^+$ or $\mathbf{9a}^{2+}$, and the ν(CO) spectra are shown in Figure 6; the spectrum for $\mathbf{9a}^+$ was confirmed by Coulometric oxidation in an OTTLE cell. The diagnostic symmetrical A_1 ν(CO) mode systematically shifts to higher energy by $\sim$27 cm^{-1} with each incremental oxidation, 2030 (**9a**), 2059 ($\mathbf{9a}^+$), and 2084 cm^{-1} ($\mathbf{9a}^{2+}$). For comparison, oxidation of the analogue with only one redox center, **10**, shifts the A_1 mode by 52 cm^{-1}, that is, almost *twice* that for **9a**. If the two equivalent (μ-alkyne)$Co_2(CO)_4$dppm redox centers were localized, the IR spectrum of a mixed-valence $\mathbf{9a}^+$ should show two A_1 ν(CO) bands; if they are electronically coupled, the A_1 band for this complex should be reduced in energy relative to a localized analogue with one redox site $\mathbf{10}^+$.

On this basis **9a** clearly has a delocalized ground state on the IR time scale. The electronic spectrum of **9a** also changes incrementally upon oxidation. New bands at 450 and 835 nm progressively increase in intensity as the concentration of $\mathbf{9a}^+$ increases with a well-defined isosbestic point (Figure 7); the band at 835 nm is lost on the formation of $\mathbf{9a}^{2+}$. It is tempting to attribute the 850 nm band to an intravalence charge-transfer transition, but it could equally arise from a change in the HOMO/SUMO composition. Unfortunately, we were unable to get a definitive ESR for $\mathbf{9a}^+$ to check whether there is spin as well as Coulombic interaction.

Conclusion

The electrochemical and spectrochemical data herein provide strong evidence that communication along a polyyne backbone to terminal molecules is not quenched by the coordination of redox-active Co_2 phosphine-substituted oxidizable subunits. Furthermore, communication does not "bypass" the cluster unit and can therefore be tuned by incorporating ligands with variable donating capability. To our knowledge **9a** provides the first example of a μ-alkyne−Co_2 complex where there is evidence for delocalization and Coulombic communication between Co_2C_2 redox centers with phosphine ligands. Whether it is a feature of dppm coordination causing a modification of the structure or subtle orbital and through-space effects (it is interesting that the distance between the centroids of the adjacent Co_2C_2 units is 3.33 Å) is unknown at present; attempts to obtain a structure of $\mathbf{9a}^+$ continue. The polyyne/cluster modules, with *one* chelated phosphine ligand per cluster, are kinetically stable upon oxidation, unlike the reducible modules, and should therefore be suitable as active components in larger arrays. Stereochemical constaints imposed by both the ligand and polyyne substituents restrict the molecular geometry. In our group these principles have been used, with adaption of the synthetic methodology, to produce larger arrays in which the polyyne/cluster modules are orientated by polyaromatic and ferrocenyl-derived spacers.

Experimental Section

Dicobalt octacarbonyl and phenylacetylene (Merck), ferrocene (Johnson and Matthey), dppm (Strem), and trimethyl

(37) Morrison, W. H.; Krogsrud, S.; Hendrickson, D. N. *Inorg. Chem.* **1973**, *12*, 1998. Shu, P.; Krogsrud, K.; Hendrickson, D. N. *Inorg. Chem.* **1976**, *41*, 1849.

(38) Levanda, C.; Bechgaard, K.; Cowan, D. O. *J. Org. Chem.* **1976**, *41*, 2700.

phosphite (Fluka) were used as received; **1a**,[39] **1b**, and {FcC≡C−}$_2$ were prepared by literature methods.[13] Solvents were dried and distilled by standard procedures, and all reactions were performed under nitrogen. IR spectra were recorded on a Digilab FX60 spectrometer, and NMR, on Varian VXR300 MHz and Gemini 200 MHz spectrometers. ^{1}H NMR were referenced to $CDCl_3$, and ^{31}P to external 85% H_3PO_4. Microanalyses were carried out by the Campbell Microanalytical Laboratory, University of Otago. FAB mass spectra were recorded on a Kratos MS80RFA instrument with an Iontech ZN11NF atom gun. Chemical oxidation for R = Ph derivatives was carried out by titrating the compound with $AgPF_6$ in CH_2Cl_2 monitored by IR. Electrochemical measurements were performed in CH_2Cl_2 using a three-electrode cell (SCE reference uncorrected for junction potentials) with a polished disk, Pt (2.27 mm^2), or GC as the working electrode; solutions were ~10^{-3} M in electroactive material and 0.10 or 0.15 M (square-wave voltammetry) in supporting electrolyte (triply recrystallized (TBA)PF_6). Data was recorded on an EG & G PAR 273A computer-controlled potentiostat. Scan rates of 0.05−10 V s^{-1} were typically employed for cyclic voltammetry, and for Osteryoung square-wave voltammetry, square-wave step heights of 1−5 mV and a square amplitude of 15−25 mV with a frequency of 30−240 Hz. A fresh solution was used for each set of conditions and agreement between experiments was excellent. Kinetic parameters were obtained from a set of data by means of the COOL algorithm. All potentials in this paper are referenced to SCE; recrystallized decamethylferrocene and sublimed ferrocene gave −0.0765 and 0.468 V, respectively. The OTTLE cell had a Pt gauze working electrode and 1 mm spacer controlled by a home-built potentiostat; the solvent was CH_2Cl_2. BPK-initiated ETC reactions were carried out as described previously.[30]

Trimethyl Phosphite Derivatives of 1a. $P(OMe)_3$ (1.5 g, 12 mmol) was added to **1a** (0.23 g, 0.3 mmol) dissolved in 40 mL of benzene. A mixture of products was obtained, the relative proportions of which depended on stirring time and thermal input. A typical product separation and characterization procedure is as follows. Solvent was removed under reduced pressure and separation achieved using preparative TLC silica plates with a CH_2Cl_2/hexane (1:1) solvent mixture giving seven bands. Band 1: red brown, R_f = 0.83, PhC≡CC_2-$Co_2(CO)_6$Ph.[13] Dark green band 2: R_f = 0.75, crystallized from chilled MeOH, **5a**; *m/e* 814 (M^+ − 2CO), corresponding peaks (M^+ − 3CO ... M^+ − 11CO), 438 [M^+ − 11CO − $P(OMe)_3$]; ^{1}H NMR ($CDCl_3$) δ 3.35 (d, $^3J_{P-H}$ = 11 Hz, 9H, −OCH_3), 7.3 (m, 6H, phenyl *H*), 7.6 (m, 4H, phenyl *H*); ^{31}P NMR ($CDCl_3$) δ 159 (s); IR (hexane) ν_{CO} 2087 (m), 2062 (vs), 2052 (vs), 2029 (s), 2023 (s), 2007 (s), 1998 (s), 1975 (w) cm^{-1}. Band 3: red brown, R_f = 0.69, crystallized from chilled MeOH, **2a**. Anal. Calcd for $C_{24}H_{19}Co_2O_8P$: C, 49.34; H, 3.28; P, 5.30. Found: C, 49.64; H, 3.27; P, 5.58. ^{1}H NMR ($CDCl_3$): δ 3.44 (d, $^3J_{P-H}$ = 12 Hz, 9H, −OCH_3), 7.3 (m, 6H, phenyl *H*), 7.5 (m, 2H, phenyl *H*), 7.7 (m, 2H, phenyl *H*). ^{31}P NMR ($CDCl_3$): δ 159 (s). IR (hexane): ν_{CO} 2072 (s), 2027 (vs), 2015 (vs), 1982 (w) cm^{-1}; $\nu_{C\equiv C}$ 2175 (vw) cm^{-1}. Dark green band 4: R_f = 0.55, an oil identified as two isomers of **6a**; *m/e* 910 (M^+ − 2CO), corresponding peaks (M^+ − 3CO ... M^+ − 10CO), 562 [M^+ − 10CO − $P(OMe)_3$]. ^{1}H NMR ($CDCl_3$): δ 3.35 (d, $^3J_{P-H}$ = 11 Hz, 18H, −OCH_3, 1st isomer), 3.38 (d, $^3J_{P-H}$ = 11 Hz, 18H′, -OCH'_3, 2nd isomer), 7.3 (m, 6H, phenyl *H*), 7.6 (m, 4H, phenyl *H*). ^{31}P NMR ($CDCl_3$): δ 161 (s). IR (hexane): ν_{CO} 2071 (s), 2053 (s), 2028 (vs), 2001 (s), 1973 (s) cm^{-1}. Red brown band 5: R_f = 0.47, crystallized from chilled MeOH, **3a**. Anal. Calcd for $C_{26}H_{28}Co_2O_{10}P_2$: C, 45.90; H 4.15; P, 9.11. Found: C, 46.09; H, 4.04; P, 9.33. MS: *m/e* 652 (M^+ − CO), corresponding peaks (M^+ − 2CO ... M^+ − 4CO), 444 [M^+ − 4CO − $P(OMe)_3$], 320 [M^+ − 4CO − 2$P(OMe)_3$]. ^{1}H NMR ($CDCl_3$): δ 3.41 (m, $^3J_{P-H}$ = 12 Hz, 18H, −OCH_3), 7.3 (m, 6H, phenyl *H*) 7.4 (m, 2H, phenyl *H*), 7.7 (m, 2H, phenyl *H*). ^{31}P NMR ($CDCl_3$): δ 163 (s). IR (hexane): ν_{CO} 2039 (vs), 1988 (vs), 1965 (w) cm^{-1}; $\nu_{C\equiv C}$ 2172 (vw) cm^{-1}. Dark green band 6: R_f = 0.33; **7a** was unstable, slowly decomposing to a mixture of **6a** and **3a**. ^{1}H NMR ($CDCl_3$): δ 3.34 (d, $^3J_{P-H}$ = 11 Hz, 9H, −OCH_3), 3.38 (d, $^3J_{P-H}$ = 11 Hz, 9H, −OCH_3), 3.67 (d, $^3J_{P-H}$ = 12 Hz, 9H, −OCH_3), 7.1−7.8 (m, 10H, phenyl *H*). ^{31}P NMR ($CDCl_3$): 160 (s), 162 (s), 166 (s). IR (hexane): ν_{CO} 2059 (m), 2026 (s), 2013 (s), 1988 (vs), 1968 (s) cm^{-1}. Red brown band 7: R_f = 0.20, **4a**; *m/e* 776 (M^+) corresponding peaks (M^+ − CO ... M^+ − 3CO), 568 [M^+ − 3CO − $P(OMe)_3$], 444 [M^+ − 3CO − 2$P(OMe)_3$], 320 [M^+ − 3CO − 3$P(OMe)_3$]; ^{1}H NMR ($CDCl_3$) δ 3.36 (m, $^3J_{P-H}$ = 11 Hz, 9H, −OCH_3) 3.40 (m, $^3J_{P-H}$ = 11 Hz, 9H, −OCH_3), 3.69 (d, $^3J_{P-H}$ = 11 Hz, 9H, −OCH_3), 7.1−7.4 (m, 8H, phenyl *H*), 7.8 (m, 2H, phenyl *H*); ^{31}P NMR ($CDCl_3$) δ 164 (m, 2P), 171 (s, 1P). IR (hexane): ν_{CO} 2010 (vs), 1969 (vs), 1951 (w) cm^{-1}; $\nu_{C\equiv C}$ 2169 (w) cm^{-1}. All products were soluble in MeOH, hexane, chlorinated and aromatic solvents.

Preparation of 8a. $Co_2(CO)_8$ (240 mg, 0.7 mmol) was added to **3a** (104 mg, 0.15 mmol) dissolved in 25 mL of benzene and stirred for 1 h at room temperature. PTLC as above gave 17 mg of **3a** and one other band, R_f = 0.6, **13a** (69 mg, 47%). Anal. Calcd for $C_{32}H_{28}Co_4O_{16}P_2$: C, 39.78; H, 2.92; P, 6.41. Found: C, 39.88; H, 2.70; P, 6.52. ^{1}H NMR ($CDCl_3$): δ 3.35 (m, $^3J_{P-H}$ = 11 Hz, 18H, −OCH_3), 7.1−7.3 (m, 6H, phenyl *H*), 7.7 (m, 4H, phenyl *H*). ^{31}P NMR ($CDCl_3$): δ 158 (s). IR (hexane): ν_{CO} 2082 (s), 2047 (vs), 2030 (s), 2023 (s), 2016 (m), 1997 (m), 1975 (s), 1964 (w) cm^{-1}.

Trimethyl Phosphite Derivatives of 1b. $P(OMe)_3$ (0.05g, 0.4 mmol) was added to **1b** (0.11 g, 0.1 mmol) dissolved in 40 mL of benzene. Products were separated as described above for the **1b** analogues. A typical product separation follows. Band 1: FcC≡C$C_2Co_2(CO)_6$Fc[13]. Dark green band 2: R_f = 0.58, **5b**; *m/e* 1086 (M^+), corresponding peaks (M^+ − 2CO ... M^+ − 11CO), 654 [M^+ − 11CO − $P(OMe)_3$]; ^{1}H NMR ($CDCl_3$) δ 3.56 (d, $^3J_{P-H}$ = 11 Hz, 9H, −OCH_3), 4.22 (s, 5H, C_5H_5) 4.26 (s, 5H, C_5H_5), 4.26−4.32 (m, 4H, C_5H_4), 4.5−4.6 (m, 4H, C_5H_4 *H*); ^{31}P NMR ($CDCl_3$) δ 157 (s); IR (hexane) ν_{CO} 2084 (m), 2057 (vs), 2047 (vs), 2026 (s), 2019 (vs), 2004 (s), 1996 (m), 1972 (w) cm^{-1}. Red brown band 3: R_f = 0.45, **2b**; *m/e* 800 (M^+), corresponding peaks (M^+ − 2CO ... M^+ − 5CO), 536 [M^+ − 5CO − $P(OMe)_3$]; ^{1}H NMR ($CDCl_3$) δ 3.53 (d, $^3J_{P-H}$ = 12 Hz, 9H, −OCH_3), 4.26 (s, 5H, −C_5H_5), 4.35 (s, 5H, −C_5H_5) 4.2−4.6 (m, 8H, C_5H_4); ^{31}P NMR ($CDCl_3$) δ 161 (s); IR (hexane) ν_{CO} 2064 (s), 2018 (vs), 2009 (vs), 1979 (w); $\nu_{C\equiv C}$ (KBr) 2173 (vw) cm^{-1}. Dark green band 4: R_f = 0.35, two isomers of **6b**; ^{1}H NMR ($CDCl_3$) δ 3.62 (d, $^3J_{P-H}$ =11Hz, 18H, −OCH_3), 3.64 (d, $^3J_{P-H}$ = 11 Hz, 18H*, −OCH_3*), 4.25 (s, 10H*, −C_5H*$_5$), 4.26 (s, 10H, −C_5H_5), 4.3 (m, 4H), 4.7 (m, 4H); ^{31}P NMR ($CDCl_3$) δ 160 (isomer *), 162 (isomer 2); IR (CH_2Cl_2) ν_{CO} 2068 (s), 2049 (s), 2024 (vs) 1990 (s) 1973 (m) cm^{-1}. The isomers were unstable in solution, decomposing to a mixture of **2b** and **5b**. Red brown band 5: R_f = 0.15, **3b**; *m/e* 896 (M^+), corresponding peaks (M^+ − CO ... M^+ − 4CO), 660 [M^+− 4CO − $P(OMe)_3$], 536 [M^+− 4CO − 2$P(OMe)_3$]; ^{1}H NMR ($CDCl_3$) δ 3.61 (m, $^3J_{P-H}$ = 12 Hz, 18H, −OCH_3), 4.23 (s, 5H, −C_5H_5), 4.24 (m, 4H), 4.35 (s, 5H, −C_5H_5), 4.24 (m, 4H), 4.35 (s, 5H, −C_5H_5), 4.43 (t, J = 1.8 Hz, 2H), 4.55 (t, J = 1.8 Hz, 2H); ^{31}P NMR ($CDCl_3$) δ 167 (s); IR (hexane) ν_{CO} 2026 (s), 1995 (vs), 1969 (vs); $\nu_{C\equiv C}$ 2147 (w) cm^{-1}. Red brown band 6: eluted with CH_2Cl_2, **4b**; *m/e* 992 (M^+), corresponding peaks (M^+ − CO ... M^+ − 3CO), 812 [M^+ − 2CO − $P(OMe)_3$], corresponding peaks [M^+ − 3CO − $P(OMe)_3$ ... M^+ − 3CO − 3$P(OMe)_3$]; ^{1}H NMR ($CDCl_3$) δ 3.6 (m, 27H, −OCH_3), 4.1−4.6 (m, 8H), 4.24 (s, 5H, − C_5H_5), 4.35 (s, 5H, −C_5H_5); ^{31}P NMR ($CDCl_3$) δ 165 (s), 168 (s) in a 2:1 ratio; IR (hexane) ν_{CO} 1998 (s), 1952 (vs); $\nu_{C\equiv C}$ 2173 (w) cm^{-1}.

Preparation of dppm Derivatives of 1a. dppm (0.30 g, 0.8 mmol) was added to **1a** (0.30 g, 0.4 mmol) dissolved in 40 mL of benzene, and the resulting solution was refluxed for 1 h. The solvent was removed under reduced pressure, and the reaction mixture was separated using preparative TLC plates (SiO_2), hexane/CH_2Cl_2 (2:1). A dark red band, R_f = 0.41, crystallized from CH_2Cl_2 layered with hexane, gave **10a** (14%

(39) Dickson, R. S.; Tailby, G. R. *Aust. J. Chem.* **1969**, *22*, 1143.

yield). Anal. Calcd for $C_{45}H_{32}Co_2O_4P_2$: C, 66.19; H, 3.95; P, 7.59. Found: C, 66.11; H 3.78; P, 7.59. ^{1}H NMR ($CDCl_3$): δ 3.22 [dt ($^2J_{H-H}$ = 14 Hz) ($^2J_{P-H}$ = 11 Hz), 1H, P−CH_2−P], 3.79 [dt ($^2J_{H-H}$ = 14 Hz) ($^2J_{P-H}$ = 11 Hz), 1H, P−CH_2−P], 7.1−7.5 (m, 28H, phenyl *H*), 7.9 (m, 2H, phenyl *H*). ^{31}P NMR ($CDCl_3$): δ 40 (s). IR (CH_2Cl_2): ν_{CO} 2024 (s), 2001 (vs), 1973 (vs), $\nu_{C\equiv C}$ 2163 (w) cm^{-1}. The other band, R_f = 0.17, crystallized from CH_2Cl_2 layered with hexane, gave green/black **9a** (39% yield). Anal. Calcd for $C_{74}H_{54}Co_4O_8P_4$: C, 62.12; H, 3.80; P, 8.66. Found: C, 61.84; H, 3.49; P, 8.50. ^{1}H NMR ($CDCl_3$): 2.98 (m, 2H, P−CH_2−P), 3.14 (m, 2H, P−CH_2P), 6.8−7.3 (m, 50H, phenyl *H*). ^{31}P NMR ($CDCl_3$): δ 39 (s). IR (CH_2Cl_2): ν_{CO} 2029 (m), 2002 (vs), 1968 (s) cm^{-1}. **11a**, R_f = 0.14, was obtained by heating **1a** or **8a** in toluene with a 3:1 excess of dppm. Separation as above gave dark red crystals from ethyl acetate. Anal. Calcd for $C_{68}H_{54}Co_2O_2P_4$: C, 71.34; H, 4.75; P, 10.82. Found: C, 71.12; H, 4.73; P, 10.77. ^{1}H NMR ($CDCl_3$): δ 3.4 (m, 2H, P−CH_2−P), 3.62 [dt ($^2J_{H-H}$ = 14 Hz) ($^2J_{P-H}$ = 11 Hz), ^{1}H, P−CH_2−P], 4.23 [dt ($^2J_{H-H}$ = 14 Hz) ($^2J_{P-H}$ = 11 Hz), 1H, P−CH_2−P], 6.6−6.8 (m, 8H, phenyl *H*), 6.9−7.4 (m, 38H, phenyl *H*), 7.6 (m, 4H, phenyl *H*). ^{31}P NMR ($CDCl_3$): δ 40, 44 (s, 1:1, 4P). IR (CH_2Cl_2): ν_{CO} 1923 (vs); $\nu_{C\equiv C}$ 2156 (w) cm^{-1}.

Preparation of dppm Derivatives of 1b. dppm (0.08 g, 0.2 mmol) was added to **1b** (0.10 g, 0.1 mmol) dissolved in 30 mL of benzene, and the resulting solution was refluxed for 0.5 h. The solvent was removed under reduced pressure, and the reaction mixture was separated on a silica column, eluting with hexane/CH_2Cl_2 (1:1). A dark red band, R_f = 0.69, crystallized from CH_2Cl_2 layered with hexane, gave 66 mg (63% yield) of **10b**. Anal. Calcd for $C_{53}H_{40}Co_2Fe_2O_4P_2$: C, 61.66; H, 3.91; P, 6.00. Found: C, 61.29; H, 3.71; P, 6.02. MS *m/e* 1032 (M^+), corresponding peaks (M^+ − CO ... M^+ − 4CO). ^{1}H NMR ($CDCl_3$): δ 3.25 [dt ($^2J_{H-H}$ = 13 Hz, $^2J_{P-H}$ = 10 Hz), 1H, P−CH_2−P], 3.73 [dt ($^2J_{H-H}$ = 13 Hz, $^2J_{P-H}$ = 10 Hz), 1H, P−CH_2−P], 4.21 (s, 5H, −C$_5H_5$, 4.30 (m, 4H), 4.39 (s, 5H, −C$_5H_5$), 4.52 (t, *J* = 1.8 Hz, 2H), 4.54 (t, *J* = 1.8 Hz, 2H), 4.54 (t, *J* = 1.8 Hz, 2H), 7.1−7.5 (m, 20H, phenyl *H*). ^{31}P NMR ($CDCl_3$): δ 38 (s). IR (CH_2Cl_2): ν_{CO} 2022 (s), 1997 (vs), 1970 (s) cm^{-1}. Elution of the second band gave a black crystalline product identified as $Co_4(CO)_8(dppm)_2$ from microanalytical, NMR, and IR data.[29]

X-ray Data Collection, Reduction, and Structure Solution for 9a. Crystals of compound **9a** were obtained as described above and crystallized from CH_2Cl_2/hexane. A green/black block was used for the data collection. Data were collected from the weakly diffracting crystals on a Siemens R3m/V, four-circle, fully automated diffractometer. Cell dimensions were derived from the angular measurements of 30 strong reflections in the range $3 < 2\theta < 25°$. Details of the crystals, data collection, and structure refinement are summarized in Table 3. Lorentz, polarization, and empirical absorption corrections were applied using the SHELXLTL system.[40] The structure was solved by direct methods using SHELXS-86;[41] the optimum electron density map revealed the location of the Co and P atoms together with the C atoms of the dialkyne chain, some of the phenyl ring C atoms, and C and O atoms of the carbonyl groups. Remaining non-H atoms were located in subsequent difference Fourier, weighted full-matrix least-squares refinement cycles using SHELXL-93.[42] Hydrogen atoms were included as fixed contributions to F_c with fixed isotropic temperature factors. The Co, P, and carbonyl O atoms were refined anisotropically due to the limitations of the data set. Attempts at additional anisotropic refinement of the alkyne C atoms led to them displaying non-positive definite temperature factors, which is most probably a consequence of difficulties with the empirical absorption correction. This model of the structure converged with $R(\sum|F_o| - |F_c|/\sum|F_o|)$ = 0.0859 ($F > 2\sigma(F)$, 2886 reflections) and w$R2 = [\sum w(F_o^2 - F_c^2)^2/\sum wF_o^4]^{1/2}$ = 0.2161 (all data), with S = 0.962, $w^{-1} = \sigma^2(F_o^2) + (0.915P)^2$, and $P = (F_o^2 + 2F_c^2)/3$. The final difference Fourier map was essentially flat with residual electron density max = 0.60 and min = −0.69 e Å^{-3}. Final positional and equivalent thermal parameters are given in Supporting Information. A full listing of bond lengths and angles, thermal parameters of the anisotropic non-hydrogen atoms, positional and thermal parameters of the the calculated H atoms, observed and calculated structure factors, and mean plane data is available from the authors (J.S.).

Table 3. Crystal Data and Structure Refinement for 9a

empirical formula	$C_{74}H_{54}Co_4O_8P_4$
fw	1430.77
temp	130(2) K
wavelength	0.710 73 Å
cryst system	monoclinic
space group	$P2_1$
unit cell dimens	a = 12.381(4) Å; b = 15.006(4) Å, β = 97.24(2)°; c = 17.134(4) Å
V	3158(2) Å^3
Z	2
D(calcd)	1.505 Mg/m^3
abs coeff	1.192 mm^{-1}
F(000)	1460
cryst size	0.42 × 0.25 × 0.22 mm
θ range for data collcn	2.14−24.00°
index ranges	$-14 \le h \le 0$, $0 \le k \le 17$, $-19 \le l \le 19$
reflcns collcd	5429
indepdt reflcns	5168 (R_{int} = 0.0845)
refinement method	full-matrix least-squares on F^2
data/restraints/params	5167/1/441
goodness-of-fit on F^2	1.026
final R indices [$I > 2s(I)$]	$R1$ = 0.0864, w$R2$ = 0.1300
R indices (all data)	$R1$ = 0.1722, w$R2$ = 0.1617
absolute struct param	0.08(4)
largest diff peak and hole	0.619 and −0.662 e Å^{-3}

Acknowledgment. We thank Professor W. T. Robinson, University of Canterbury, for the X-ray data collection and Dr. B. Clark, University of Canterbury, for the mass spectra.

Supporting Information Available: Full tables of bond length and angle data, anisotropic thermal parameters, and atom positional and thermal parameters (7 pages). Ordering information is given on any current masthead page.

OM9602769

(40) Sheldrick, G. M. An integrated system for solving, refining and displaying crystal structures from diffraction data, SHELXTL.

(41) Sheldrick, G. M. A program for the solution of crystal structures from diffraction data, University of Gottingen. Sheldrick, G. M. *Acta Crystallogr.* **1990**, *A46*, 467.

(42) Sheldrick, G. M. SHELXL-93. J. *Appl. Crystallogr.* **1993**, in preparation.